INTERPLAY OF COMPUTATIONAL CHEMISTRY AND TRANSIENT ABSORPTION SPECTROSCOPY IN THE ULTRAFAST STUDIES

© 2007　**E.A. Pritchina[1,2], N.P. Gritsan[1,2]*, G.T. Burdzinski[3,4], M.S. Platz[4]**

[1]*Institute of Chemical Kinetics and Combustion SB RAS, Novosibirsk, Russia*
[2]*Novosibirsk State University, Novosibirsk, Russia*
[3]*Quantum Electronics Laboratory, Faculty of Physics, Adam Mickiewicz University, Poznan, Poland*
[4]*Department of Chemistry, The Ohio State University, Columbus, Ohio, USA*

The primary physical and chemical processes in the photochemistry of 1-(trideuteromethyl)-2,3,4-trideutero (**1**) and 1-acetoxy-2-methoxy- (**2**) 9,10-anthraquinones were studied using femtosecond transient absorption spectroscopy and computational chemistry. Excitation of **1** and **2** at 270 nm results in the population of a set of highly excited singlet states which decay within the laser pulse by internal conversion and vibrational energy redistribution. The transient absorption spectra of the lowest singlet and triplet excited states of substituted anthraquinones **1** and **2** as well as the triplet excited and ground states of the products were detected. The assignments of the transient absorption spectra were performed on the basis of quantum chemical calculations of the electronic absorption spectra of the intermediates. Time-dependent density functional theory or CASSCF/CASPT2 procedure were used to calculate the spectroscopic properties of the intermediates.

K e y w o r d s: femtosecond transient absorption spectroscopy, photochemical hydrogen transfer, photochemical acyl migration, electronic absorption spectra calculations, time-dependent density functional theory, CASSCF/CASPT2 procedure.

INTRODUCTION

There has been recent, dramatic progress in the development and application of computational methods in chemistry. To a great extent this is a result of the astonishing and unprecedented development of digital computer technology. Computational chemists have taken advantage of this progress to develop a number of new theoretical approaches and techniques and to build up a broad array of new theoretical tools. The synergy between theory and experiment leads to the acceleration and improvement of a number of areas of chemistry. For example, the field of the matrix isolation spectroscopy is now always accompanied with theoretical calculations of IR and UV-Vis spectra of proposed reactive intermediates [1, 2]. Quantum chemistry has been also extensively used for understanding and interpretation of the properties of reactive intermediates [3], including whose generated upon laser flash photolysis [4].
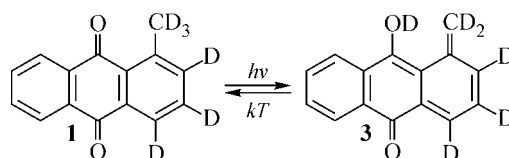
However, computational methods have been infrequently applied to the interpretation of the results of ultrafast studies in the femto- and picosecond time domains. This is caused, in part, by the fact that excited state intermediates are usually the only species detected on this time scale. Open-shell species are the most challenging molecules for quantum chemical calculations and require multi-configuration approaches. It is even harder to calculate the UV-Vis spectra of such species. It should be noted that the reported transient absorption spectra of different intermediates are often strongly overlapped, thus quantum chemical calculations can give invaluable information for a proper

---

assignment and interpretation. One commonly accepted method for the calculation of the properties of open-shell species including their UV-Vis spectra is the CASSCF/CASPT2 procedure [5] available in the MOLCAS program [6]. Much less is known about the application of a new technique — EOM-SF-CCSD (spin-flip equation-of-motion coupled-cluster electronic structure method) [7] realized in Q-CHEM suite of programs [8]. It is clear that both techniques require huge computer resources and could be applied only for small and moderate size systems, a happy exception is only the case of highly symmetrical species.
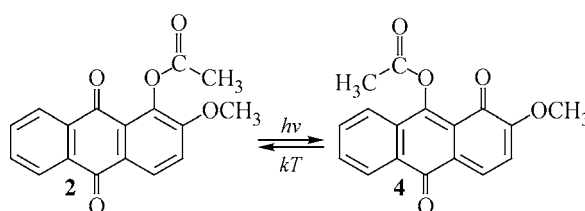
This paper will demonstrate the power of UV-Vis spectral calculations for excited state intermediates to confidently assign the transient absorption spectra detected on the femto- and picosecond time scales after femtosecond excitation of 1-(trideuteromethyl)-2,3,4-trideuterio-anthraquinone (**1**, Scheme 1) and 1-acetoxy-2-methoxyanthraquinone (**2**, Scheme 2). All experimental details and analysis of the complicated kinetic schemes supported by the results of these quantum chemical calculations will be published elsewhere.

It should be noted, that in contrast to very fast proton transfer (~50 fs) [9] much less is known about primary processes in hydrogen atom transfer reactions. Earlier [10] we found that in the case of 1-methylanthraquinone and its deuteron analogue (**1**) the photochemical transfer of a hydrogen and deuterium atom occurs in both singlet and triplet excited states and yields the 9-hydroxy-1,10-anthraquinone-1-methide or its deuteron analogue (**3**, Scheme 1) as a final product. However, the resolution of the system (~30 ns) was not sufficient to study the dynamics of these processes.

Scheme 1

Migration of bulky polyatomic groups is an even less well studied process. A photochemical acyl group migration has been observed for a series of 1-acetoxy-9,10-anthraquinone derivatives [11]. It was found that photochemical acyl group migration is a concerted adiabatic process occurring on the triplet potential energy surface (PES) [12, 13]. It should be noted, that most known photochemical reactions proceed non-adiabatically through conical intersections [14]. Much less is known about adiabatic photochemical reactions, especially those occurring on a triplet PES.

Scheme 2

A series of O-acyl derivatives of 1-hydroxy-2-methoxyanthraquinone were studied using nanosecond laser flash photolysis [13]. In the case of electron donating substituents in the migrating carbonyl group the short-lived intermediates were tentatively assigned to the triplet excited states of the *para*-quinones. However, the time resolution of the system (~3 ns) was not sufficient to observe acetoxy group migration nor to study the dynamics of the primary photophysical processes [13].

In this work we have applied ultrafast transient absorption spectroscopy technique to monitor the migration of deuterium and acetoxy group upon excitation of anthraquinones **1** and **2**, respectively. To assign the transient absorption spectra the UV-Vis spectra of the proposed excited state intermediates were calculated using time-dependent density functional theory or CASSCF/CASPT2 method.

EXPERIMENTAL AND COMPUTATIONAL DETAILS

Femtosecond broadband UV-Vis transient absorption experiments. Ultrafast studies were performed at the Ohio State University Center for Chemical and Biophysical Dynamics. Transient absorption spectra were recorded on a femtosecond broadband UV-Vis transient absorption spectrometer [15] in acetonitrile at room temperature at an excitation wavelength of 270 nm. Transient absorption spectra were registered at different pump-probe delay times using an optical delay line. The instrument response (fwhm) was approximately 300 fs.

Nanosecond laser flash photolysis (LFP). An eximer XeCl laser (Lambda Physik, 308 nm, 20 ns, 50 mJ) was used as the excitation light source. The spectrometer has been described previously [16].

Quantum chemical calculations. The geometries of the ground singlet and lowest triplet states of substituted 9,10-anthraquinones (**1, 2**) and 1,10-anthraquinones (**3, 4**) were calculated at the (U)B3LYP [17, 18] level of theory with the 6-31G(*d,p*) basis set, using the Gaussian-03 suite of programs [19]. All equilibrium structures were ascertained to be minima on the potential energy surfaces and the stability of the SCF solutions was tested. The influence of solvent on the energies of stationary and transition points was taken into consideration by the PCM [20] models as implemented to Gaussian-03.

To predict the electronic absorption spectra of the ground state reactants and products and of the intermediates in the lowest triplet excited states the time-dependent (TD) DFT method [21] with the B3LYP combination of exchange [17] and correlation [18] functionals was used with the 6-31+G(*d,p*) basis set.

Excited state energies of 9,10-anthraquinone (which serves as model of compound **1**) were calculated at the CASSCF/6-31G(*d*) geometries by the CASSCF/CASPT2 procedure [5] with the ANO-S basis set of Pierloot et al. [23] using the MOLCAS program [6] under limiting conditions of D_{2h}-symmetry. In order to arrive at a satisfactory description of all excited states at the CASPT2 level (i.e. to remove intruder states) it was necessary to resort to the level-shifting technique [24], whereby it was carefully ascertained that no artifacts are introduced. The active space used in these calculations is described in the text and depicted in Fig. 3.

RESULTS AND DISCUSSION

Fig. 1 demonstrates that electronic absorption spectra of **1** and **2** calculated using time-dependent density functional theory (open and solid bars, respectively) are in good agreement with experimental ones. The spectrum of **1** has very intense narrow band with maximum at 252 nm, a small feature at 272 nm, long-wavelength band with maximum at 333 nm and a low intense shoulder at 380—420 nm. The calculations predict that this shoulder is caused by two transitions to the lowest excited singlet $n\pi^*$ states (λ_{calc} = 389 and 426 nm). In the vicinity of excitation wavelength (270 nm) there are two transitions with high oscillator strength at 277 ($S_0 \rightarrow S_7$) and 246 nm ($S_0 \rightarrow S_{10}$).

The calculations predict that the lowest singlet excited state of **2** is the $^1n\pi^*$ state; transition to this state (λ_{max}(calc) = 423 nm) has very low intensity (f = 0.002) and is masked by more intense $S_0 \rightarrow S_2$ band ($\pi\pi^*$ transition, λ_{max}(exp) = 362 nm, λ_{max}(calc) = 387 nm, f = 0.07). In the vicinity of excitation wavelength (270 nm) **2** has three
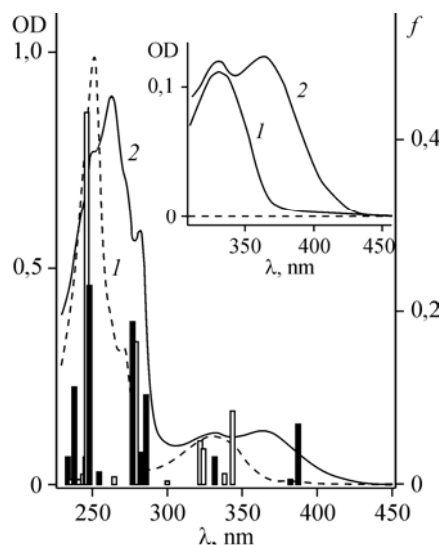

Fig. 1. Electronic absorption spectra of 1-(trideuteromethyl)-2,3,4-trideuterio-anthraquinone (**1**, spectrum *1*) and 1-acetoxy-2-methoxyanthraquinone (**2**, spectrum *2*) in acetonitrile (C = 2×10^{-5} M). The vertical bars indicate the positions and oscillator strengths (f) of the electronic transitions calculated for **1** (open bars) and **2** (solid bars) in ground state by the TD-B3LYP/6-31+G(*d,p*) technique
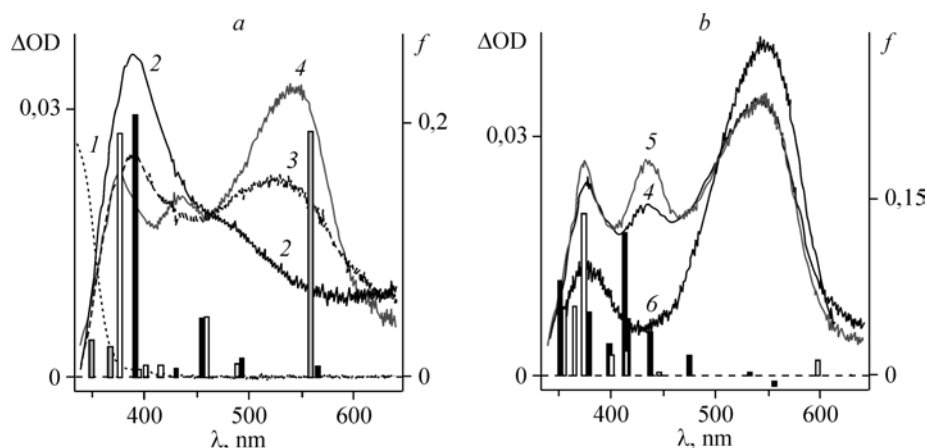
Fig. 2. The transient absorption spectra recorded:

a — after femtosecond laser excitation of 1-(trideuteromethyl)-2,3,4-trideuteroanthraquinone (**1**) in acetonitrile at 1 ps (*2*), 5 ps (*3*) and 30 ps (*4*); *1* — the UV-Vis spectrum of **1** in the ground state. The vertical bars indicate the positions and oscillator strengths (*f*) of the electronic transitions calculated for 9,10-anthraquinone in the excited singlet (solid bars) and triplet (open bars) $n\pi^*$ states by CASSCF(16,14)/CASPT2 procedure with ANO-S basis set; *b* — at 30 ps (*4*), 700 ps (*5*) and 500 ns (*6*) after excitation of **1**. The vertical bars indicate the positions and oscillator strengths (*f*) of the electronic transitions calculated for **3** in triplet excited $\pi\pi^*$ state (solid bars) and for hypothetical $\sigma\pi$-biradical (open bars) by TD-UB3LYP/6-31+G(*d,p*) technique

transitions with large oscillator strength: at 285 ($S_0{\to}S_7$), 277 ($S_0{\to}S_9$) and 248 nm ($S_0{\to}S_{11}$). Therefore, femtosecond laser excitation at 270 nm of both **1** and **2** results in the population of a set of highly excited singlet states.

Fig. 2, *a* demonstrates the immediate formation of a broad transient absorption (spectrum 2) with a maximum at 390 nm and shoulder at ~470 nm after femtosecond excitation of quinone **1**. It is reasonable to assign this transient absorption to the lowest singlet $^1n\pi^*$ excited state of **1**.

It is clear that methyl substituent only slightly influences the electronic structure of **1**. Therefore, to prove the assignment we calculated spectrum of unsubstituted anthraquinone in the singlet $^1n\pi^*$ state using CASSCF/CASPT2 procedure. First of all, the geometries of **1** in the lowest singlet and triplet $n\pi^*$ excited states as well as in the ground state were optimized at CASSCF(12,12)/6-31G(*d*) level with an active space which consisted of 11π orbitals and one non-bonded oxygen orbital — $9b_{3g}$. Fig. 3 demonstrates 14 orbitals used in the CASSCF/CASPT2 spectral calculations; the same orbitals with the exception of two of them ($1b_{2g}$ and $11b_{2u}$) were used in geometry optimization. As expected, the optimized geometries of singlet and triplet $n\pi^*$ states (Fig. 4) are very similar and differ noticeably from that of a ground state anthraquinone.

Vertical excitation energies calculated at the singlet excited $n\pi^*$ state geometry (1^1B_{1g}) by the CASPT2 method as well as oscillator strengths for these transitions are presented in Table 1 and displayed as black bars in Fig. 2, *a*. Fig. 2, *a* and Table 1 demonstrate that calculated spectrum of **1** in the $^1n\pi^*$ excited states ($^1\mathbf{1}^*$) agrees very well with the transient absorption spectrum detected at 1 ps after the laser pulse which strengthens our proposed assignment.
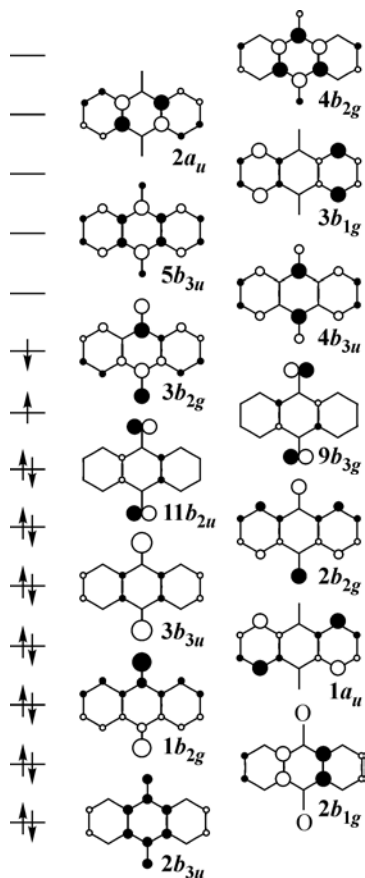

Fig. 3. Orbitals involved in the electronic transitions of the singlet and triplet antraquinone (cf. Table 1)
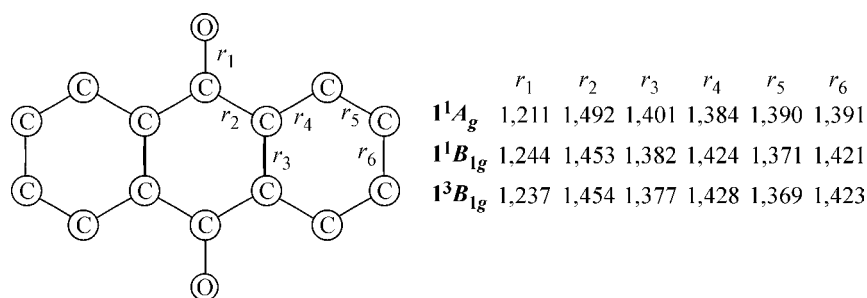
	r_1	r_2	r_3	r_4	r_5	r_6
1^1A_g	1,211	1,492	1,401	1,384	1,390	1,391
1^1B_{1g}	1,244	1,453	1,382	1,424	1,371	1,421
1^3B_{1g}	1,237	1,454	1,377	1,428	1,369	1,423

Fig. 4. Geometries (bond lengths in Å) of anthraquinone in the ground (1^1A_g) and in the lowest singlet (1^1B_{1g}) and triplet (1^3B_{1g}) excited $n\pi^*$ states optimized by CASSCF(12,12)/6-31G(*d*) method

The spectrum of **1** in the $^3n\pi^*$ excited state (^{3}**1***) was calculated in the same manner and is also displayed in Fig. 2 (open bars). The calculated spectra of singlet and triplet excited $n\pi^*$ intermediates are very similar which is reasonable upon taking into account the similar electronic nature and close

T a b l e   1

Vertical excitation energies calculated for anthraquinone in the singlet excited $n\pi^*$ state (1^1B_{1g}) by the CASPT2 method based on a CASSCF(16,14)/ANO-S wavefunction at the CASSCF(12,12)/6-31G(d) geometry [a]

State	ΔE_{CASSCF}, eV	ΔE_{CASPT2}, eV	λ, nm	f [b]	Major configurations [c]
1^1B_{1g}	0,00	0,00	–	–	54 % of $n\pi^*$ configuration (Fig. 3)
					+13 % [$3b_{2g}{\to}9b_{3g}+11b_{2u}{\to}4b_{3u}$]
1^1A_u	0,063	0,054	22793	$1,1{\times}10^{-3}$	53 % $11b_{2u}{\to}9b_{3g}$
					+13 % [$9b_{3g}{\to}4b_{3u}+3b_{2g}{\to}9b_{3g}$]
2^1B_{1g}	2,55	1,82	682	0,0	28 % [$3b_{2g}{\to}9b_{3g}+11b_{2u}{\to}4b_{3u}$]
					−18 % [$11b_{2u}{\to}3b_{2g}+3b_{3u}{\to}9b_{3g}$]
					+14 % $2b_{2g}{\to}3b_{2g}$
2^1A_u	2,55	1,88	660	$9,3{\times}10^{-4}$	29 % [$9b_{3g}{\to}4b_{3u}+3b_{2g}{\to}9b_{3g}$]
					−18 % [$9b_{3g}{\to}3b_{2g}+3b_{3u}{\to}9b_{3g}$]
1^1B_{3u}	3,39	2,19	566	$9,0{\times}10^{-3}$	24 % [$9b_{3g}{\to}2a_u + 3b_{2g}{\to}9b_{3g}$]
					−22 % [$11b_{2u}{\to}9b_{3g} + 2b_{1g}{\to}3b_{2g}$]
2^1B_{3u}	3,90	2,42	512	$3,7{\times}10^{-4}$	22 % [$3b_{2g}{\to}3b_{1g}+11b_{2u}{\to}9b_{3g}$]
					−14 % [$9b_{3g}{\to}3b_{2g}+1a_u{\to}9b_{3g}$]
3^1A_u	4,01	2,52	493	$1,5{\times}10^{-2}$	17 % [$9b_{3g}{\to}5b_{3u}+3b_{2g}{\to}9b_{3g}$]
4^1A_u	4,72	2,71	457	$4,7{\times}10^{-2}$	28 % [$11b_{2u}{\to}9b_{3g}+2b_{2g}{\to}3b_{2g}$]
					−13 % $2b_{2g}{\to}4b_{3u}$
					−12 % [$9b_{3g}{\to}4b_{3u}+3b_{2g}{\to}9b_{3g}$]
3^1B_{3u}	5,04	2,89	431	$7,4{\times}10^{-3}$	22 % [$9b_{3g}{\to}2a_u+3b_{2g}{\to}9b_{3g}$]
					+21 % [$9b_{3g}{\to}3b_{2g}+1a_u{\to}9b_{3g}$]
4^1B_{3u}	5,42	3,16	392	$2,1{\times}10^{-1}$	22 % [$2b_{1g}{\to}3b_{2g}+11b_{2u}{\to}9b_{3g}$]
					−17 % [$9b_{3g}{\to}3b_{2g}+1a_u{\to}9b_{3g}$]
					−15 % [$9b_{3g}{\to}2a_u+3b_{2g}{\to}9b_{3g}$]

[a] All states were calculated with a level shift of 0.3 h.; weights of the zero-order CASSCF in the CASPT2 wavefunctions were 0.61—0.63.

[b] Oscillator strength for electronic transition.

[c] Electron excitations within the active space of orbitals depicted in Fig. 3.

geometry (see Fig. 4) of these species. The triplet-triplet absorption spectrum of anthraquinone is known from the literature [25]; it represents a broad absorption band with maximum at 370 nm and a shoulder at ~450 nm in perfect agreement with our calculations.

The decay of $^1\mathbf{1^*}$ on the picosecond time scale is accompanied by the formation of a product **3** (Scheme 1) in the ground state which is characterized by a transient absorption in the visible region with maximum at 545 nm (see Fig. 2, *a*, spectra *3* and *4*). However, the kinetics of the $^1\mathbf{1^*}$ decay and the formation of **3** are not simply exponential, but could only be fitted to a biexponential function (details will be published elsewhere). We propose that deuterium transfer proceeds in the hot $^1n\pi^*$ state (in competition with vibrational cooling) significantly faster ($\tau = 2.5\pm0.5$ ps) than in the vibrationally cooled state ($\tau = 9\pm1$ ps). The latter process competes with the intersystem crossing to the triplet excited $n\pi^*$ state since about 45 % of product **3** arises on the nanosecond time scale from the triplet state reaction [10].

This assumption also agrees well with the spectral changes. The fast growth of absorption of **3** at 545 nm (see Fig. 2, *a*, spectrum *3*) is accompanied by significant decay at 390 nm, since **3** has very low transient absorption at this region (see Fig. 2, *b*, spectrum *6*). At the same time the slower growth at 545 nm (see Fig. 2, *a*, spectrum *4*) is accompanied by only a slight decay at 390 nm. This is the result of the formation of $^3n\pi^*$ which has a spectrum similar to that of $^1n\pi^*$ (see Fig. 2, *a*, solid and open bars). Therefore transient absorption spectrum *4* in Fig. 2, *a* belongs mainly to **3** in the ground state (absorption bands with maxima at 375 and 545 nm) and **1** in the $^3n\pi^*$ state. A small amount of the product in the triplet excited state ($^3\mathbf{3^*}$, 375 and 435 nm) is also formed on a 30 ps time scale.

At longer delay times the 545 nm band does not change (see Fig. 2, *b*, spectra *4* and *5*), but the reaction proceeds on the triplet PES. Due to the transition from $^3\mathbf{1^*}$ to $^3\mathbf{3^*}$ two new maxima at 375 and 435 nm are formed with a time constant of 100 ps. Subsequently, the increase of the **3** population is observed upon the decay of $^3\mathbf{3^*}$ (see Fig. 2, *b*, spectrum *6*).

The latter process was studied in detail in our previous paper [10]. We proposed [10] that $^3\mathbf{3^*}$ has the electronic structure of a σ,π-biradical with the plane of CH_2-methide group perpendicular to the anthraquinone ring. This assumption was based on simple AM1 calculations and was accepted in the following study [26]. Using AM1 method we optimized two minima on the triplet PES of **3**: above mentioned triplet σ,π-biradical and triplet $\pi\pi^*$ excited state of **3** with CH_2 group in the plane of anthraquinone [10].

However, using more contemporary calculations, viz. density functional theory at UB3LYP/6-31G(d,p) level, we were able to localize only one minimum on the triplet PES — $^3\pi\pi^*$ state of **3**. Moreover, we calculated triplet-triplet absorption spectrum (see Fig. 2, *b*, black bars) of **3** which coincides well with the absorption bands with maxima at 375 and 435 nm.

Nevertheless, we partially optimized structure of the hypothetical triplet σ,π-biradical keeping the CH_2 group in the plane perpendicular to the anthraquinone ring. Triplet-triplet absorption spectrum of this species is presented in Fig. 2, *b* (open bars) and does not agree with the experimental spectrum.

Therefore, though the recorded transient absorption spectra of different intermediates are strongly overlapped, the quantum chemical calculations gave us opportunity to establish the entire mechanism of very complicated primary physical and chemical processes in the photochemistry of 1-methylanthraquinone.

Transient absorption spectroscopy of 1-acetoxy-2-methoxyanthraquinone (2). The transient absorption spectra recorded over a 0—50 ps and 30—270 ns time windows after laser excitation of **2** are displayed in Fig. 5, *a*, *b*. Fig. 5, *a* demonstrates formation of a broad transient absorption with maximum at ~430 nm within the laser pulse. This band is assigned to **2** in the lowest singlet excited state ($^1\mathbf{2^*}$), presumably of the $^1n\pi^*$ type.

The decay of $^1\mathbf{2^*}$ on the picosecond time scale ($\tau = 11\pm1$ ps) is accompanied by the formation of a species with two absorption maxima at 465 and 580 nm (see Fig. 5, *a*, spectrum *2*). Similar two maxima in the range 400—650 nm were detected immediately after laser excitation (355 nm, 3 ns) of 1-acyloxy-2-methoxyanthraquinones with donor substituents in the migrating acyl and were tentatively assigned to their triplet-triplet (T-T) absorption [13].
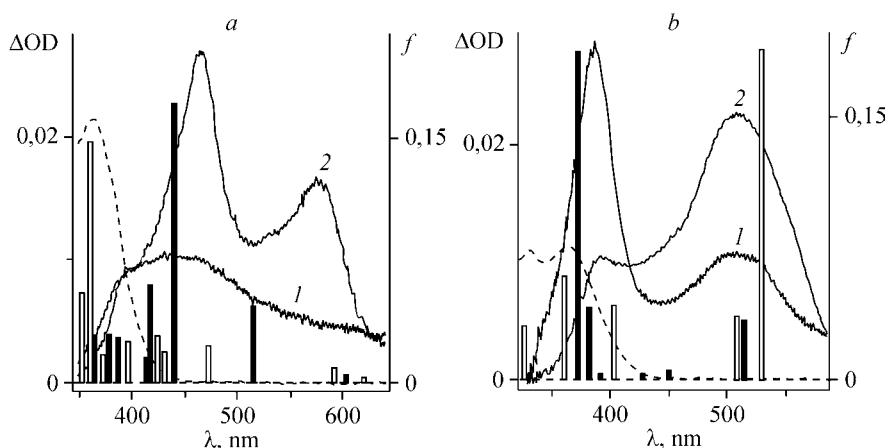
Fig. 5. The transient absorption spectra recorded in acetonitrile:
a — at 0,6 ps (*1*) and 50 ps (*2*) after femtosecond laser excitation, and *b* — at 30 ns (*1*) and 270 ns (*2*) after nanosecond laser excitation of 1-acetoxy-2-methoxyanthraquinone (**2**). The vertical bars indicate the positions and oscillator strengths (*f*) of the electronic transitions calculated: *a* — for **2** in the triplet excited states of the $\pi\pi^*$ (black bars) and $n\pi^*$ (open bars) types; *b* — for **4** in the triplet excited (black bars) and ground (open bars) states by TD-(U)B3LYP/6-31+G(*d,p*) technique. The dotted line represents the absorption spectrum of **2** in the ground state

Calculations predict that two lowest excited triplet states of **2** ($^3n\pi^*$ and $^3\pi\pi^*$) are very close in energy with $^3n\pi^*$ being slightly lower (6.1 kJ/mol) in gas phase and higher (12.1 kJ/mol) in acetonitrile. According to the orbital symmetry conservation principle only $^3\pi\pi^*$ excited state can undergo acyl migration [12], therefore this state likely to be the lowest excited state of **2**. Indeed, calculated T-T spectrum for $^3\pi\pi^*$ state (see Fig. 5, *a*, solid bars) agrees much better with experiment than that for $^3n\pi^*$ (open bars). Although both most intense transitions (440 and 515 nm) are noticeably blue-shifted from the experimental maxima (465 and 580 nm), agreement between experimental and calculated spectra of $^3\pi\pi^*$ is quite good.

Therefore, on a time scale of tens of picoseconds we detected the formation of the lowest $^3\pi\pi^*$ state of **2** (^{3}**2**) due to intersystem crossing from the excited singlet $n\pi^*$ state. The decay of ^{3}**2** ($\tau_{dec} = 220\pm30$ ps) is followed by the formation of a new species with absorption maxima at 390, ~510 nm (see Fig. 5, *b*, spectrum *1*). This spectrum was detected previously [13] and assigned to T-T absorption of the *ana*-quinone ^{3}**4**. Indeed, calculated spectrum of ^{3}**4** (see Fig. 5, *b*, solid bars) agrees perfectly with the transient absorption spectrum detected at 30 ns after the laser pulse.

Note, that the transient absorption spectra are displayed in Fig. 5. However, for comparison with calculations the contribution from bleaching of **2** should be taken into account. This is possible if one knows the extinction coefficients of **2** and **4** with the assumption that photoexcitation of **2** leads to **4** with a quantum yield close to unity. Using the extinction coefficients of **4** at 510 nm (1.1×10^4 M^{-1} cm^{-1} [12, 13]) we consecutively estimated extinction coefficients of all proposed intermediates (Table 2). It is clear that bleaching of **1a** is significant at $\lambda < 420$ nm and negligible at longer wavelengths (see Fig. 5).

T a b l e   2

*Extinction coefficient at the maximum of $S_0 \rightarrow S_2$ transition of **1a** and estimated values (accuracy ±10—15 %) of the extinction coefficients for all detected intermediates in acetonitrile*

Compound/intermediate	**2**	**^{1}2***	**^{3}2***	**^{3}4***	**4** [12, 13]
λ_{max}, nm	362	~375 [a]	580; 465	500	510
ε, M^{-1} cm^{-1}	6.3×10^3	~7.3×10^3	7.2×10^3; 1.2×10^4	3.6×10^3	1.1×10^4

[a] Bleaching of **1a** was taken into account.

Decay of the transient absorption of ^{3}**4** was accompanied by the formation of the final product **4** (see Fig. 5, *b*, spectrum *2*), which in turn reverts to **2** on the microsecond time scale by thermal acetoxy group migration [12, 13]. Fig. 5, *b* demonstrates that spectrum of *ana*-quinone **4** is also very well reproduced by the theory (but again the bleaching of **1a** affects UV part of the transient absorption spectrum).

CONCLUSION

A comprehensive, quantitative mechanism of the physical and chemical processes which follow photoexcitation of substituted anthraquinones **1** and **2** was established using femto- and nanosecond transient absorption spectroscopy. All assignments of the transient absorption spectra reported in this paper were secured by quantum chemical calculations. We demonstrated that theoretical methods can now routinely be utilized to simulate the electronic absorption spectra of the reactive intermediates detected in the ultrafast studies including excited state.

REFERENCES

1. *Maltsev A., Bally T., Tsao M.-L. et al.* // J. Amer. Chem. Soc. – 2004. – **126**. – P. 237 – 249.
2. *Gritsan N.P., Pritchina E.A., Bally T. et al.* // J. Phys. Chem. A. – 2007. – **111**. – P. 817 – 824.
3. *Borden W.T.* // In: Reactive intermediate chemistry / Eds. R.A. Moss, M.S. Platz, M. Jones. – Hoboken, NJ: John Wiley & Sons, 2004. – P. 961 – 1004.
4. *Gritsan N.P., Platz M.S., Borden W.T.* // In: Computational Methods in Photochemistry / Ed. A.G. Kutateladze. – Boca Raton: Talor & Francis, 2005. – P. 235 – 356.
5. *Andersson K., Roos B.O.* Advanced Series in Physical Chemistry, 2. Modern Electronic Structure Theory. – Singapore: World Scientific Publishing Co, 1995. – Part 1. – P. 55 – 109.
6. *Andersson K., Blomberg M.R.A., Fülscher M.P. et al.* // MOLCAS, Versions 5, Lund: University of Lund, 2002.
7. *Krylov A.I.* // Acc. Chem. Res. – 2006. – **39**. – P. 93 – 91.
8. *Shao Yi., Molnar L.F., Jung Yo.* // Phys. Chem. Chem. Phys. – 2006. – **8**. – P. 3172 – 3191.
9. *De Vivie-Riedle R., De Waele V., Kurtz L. et al.* // J. Phys. Chem. – 2003. – **107**. – P. 10591 – 10599.
10. *Gritsan N.P., Khmelinski I.V., Usov O.M.* // J. Amer. Chem. Soc. – 1991. – **113**. – P. 9615 – 9620.
11. *Gritsan N.P., Russkikh S.A., Klimenko L.S. et al.* // Teor. Eksp. Khim. – 1983. – **19**. – P. 455 – 462.
12. *Gritsan N.P., Klimenko L.S., Shvartsberg E.M. et al.* // J. Photochem. Photobiol. A: Chem. – 1990. – **52**. – P. 137 – 156.
13. *Gritsan N.P., Kellmann A., Tfibel F. et al.* // J. Phys. Chem. A. – 1997. – **101**. – P. 794 – 801.
14. *Bernardi F., Olivucci M., Robb M.A.* // Chem. Soc. Rev. – 1996. – **25**. – P. 321 – 328.
15. *Burdzinski G., Hackett J.C., Wang J. et al.* // J. Amer. Chem. Soc. – 2006. – **128**. – P. 13402 – 13411.
16. *Tsao M.-L., Gritsan N.P., James T.R. et al.* // Ibid. – 2003. – **125**. – P. 9343 – 9358.
17. *Becke A.D.* // J. Chem. Phys. – 1993. – **98**. – P. 5648 – 5652.
18. *Lee C., Yang W., Parr R.G.* // Phys. Rev. B. – 1988. – **37**. – P. 785 – 789.
19. *Frisch M.J., Trucks G.W., Schlegel H.B. et al.* // Gaussian-03, Revision C.02. – Gaussian, Inc., Wallingford C.T., 2004.
20. *Tomasi J., Mennucci B., Cammi R.* // Chem. Rev. – 2005. – **105**. – P. 2999 – 3093.
21. *Dreuw A., Head-Gordon M.* // Ibid. – P. 4009 – 4037.
22. *Roos B.O.* // Adv. Chem. Phys. – 1987. – **69**. – P. 339 – 445.
23. *Pierloot K., Dumez B., Widmark P.-O. et al.* // Theor. Chim. Acta. – 1995. – **90**. – P. 87 – 114.
24. *Roos B.O., Andersson K., Fülscher M.P. et al.* // J. Mol. Struct. (Theochem). – 1996. – **388**. – P. 257 – 276.
25. *Nakayama T., Ushida K., Hamanoue K. et al.* // J. Chem. Soc. Faraday Trans. – 1990. – **86**. – P. 95 – 103.
26. *Nakayama T., Torii Yu., Nagahara T. et al.* // J. Phys. Chem. A. – 1999. – **103**. – P. 1696 – 1703.